Technical Report # MBS2022-5-UIC
Department of Mechanical and Industrial Engineering
University of Illinois at Chicago

December 2022

SPATIAL-DYNAMICS FORMULATION OF THE *L*/*V* RATIO

Ahmed A. Shabana (shabana@uic.edu)
Department of Mechanical and Industrial Engineering
University of Illinois at Chicago
842 West Taylor Street
Chicago, Illinois 60607

ABSTRACT

Nadal's L/V limit, which is based on quasi-static planar analysis, was used to develop derailment criteria; where L and V are, respectively, lateral and vertical forces acting on railroad wheel flange. This paper describes new spatial L/V dynamic formulation based on the assumptions of Nadal's limit. The spatial analysis, which leads to simple L/V ratio that demonstrates limitations of the planar analysis, employs *non-generalized coordinates* and is independent of the bank angle that defines the track super-elevation. The single-degree-of-freedom wheel-climb model developed accounts for curving behavior, track super-elevation, and centrifugal and Coriolis inertia forces; and can be used to develop an *inverse problem* to study different wheel climb patterns. It is demonstrated that the wheel absolute acceleration is not in general zero for zero climb acceleration as in the planar analysis, and the lateral force L and vertical force V depend on quadratic-velocity inertia forces. The condition of zero absolute acceleration and non-zero climb acceleration is defined. It is shown that the spatial L/V limit can approach four if the direction of the friction force is properly accounted for, highlighting the need for accurate measurement of the components of the relative velocity at the wheel/rail contact point to have proper interpretation and use of the wheel-climb criteria. The proposed approach can be used to develop real-time onboard-computer *positive-train-control* (PTC) algorithms that define wheel-climb pattern using online measurements. Such PTC algorithms can contribute to avoiding derailments caused by wheel climb during curve negotiations.

Keywords: Wheel climb; L/V ratio; Nadal's limit; wheel/rail flange contact; non-generalized coordinates.

1. INTRODUCTION

The two railroad-derailment mechanisms most likely to occur are *wheel climb* and *wheel lift*. The wheel lift is more common during hunting oscillations on tangent tracks. Severe hunting leads to high lateral velocity, large roll moment, and impulsive wheel/rail contact forces that may lead to derailments. In this case, resultant tangential force or roll moment at one wheel can be downward due to the wheel lift at the other wheel [1, 2]. On the other hand, wheel-flange climbs, more common during curving and can occur at low velocity, are associated with large angle of attack α_a ($\alpha_a \approx 3°$). During wheel climb, the direction of the friction force acting on the wheel flange is defined by the relative-velocity direction and not by acceleration direction; forces are directly associated with accelerations and positive acceleration does not always imply positive velocity.

The (L/V) ratio, where L and V are, respectively, lateral and vertical forces acting on the wheel flange at the contact point with the rail, has been used to develop several railroad derailment criteria. Derailments are assumed to occur if this ratio, which has its roots in *Nadal's formula* introduced more than a century ago, exceeds a certain limit. The (L/V)-based criteria are concerned with *wheel climb* during curve negotiation characterized by large angle of attack. Nonetheless, a planar analysis is used to define Nadal's formula, which can be derived using *geometric approach* or quasi-static force balance. In the geometric/static approach, a coordinate transformation is used to write the lateral and vertical forces in terms of the normal-reaction and friction forces without considering velocity-dependent inertia forces. The L and V forces are interpreted as force resultant acting on the wheel flange excluding constraint and friction forces at the contact point. The assumption used by Nadal, that direction of friction force in its totality is tangent to the flange neglecting longitudinal friction-force component, is investigated in this study by relaxing the planar-analysis assumptions.

Nadal's L/V ratio is defined in terms of the flange angle α and the coefficient of friction μ as $L/V = \left(\tan\alpha - \mu\right)/\left(1 + \mu\tan\alpha\right)$. This equation is not function of the angle of attack α_a or the wheel yaw angle and is used, as reported in the literature, to conclude that for a given α, an increase of μ leads to a decrease of Nadal's limit. That is, increasing μ is associated with a decrease in L for given V regardless of the magnitude of α; and in the special case in which $\mu = 0$, one has $\left(L/V\right) = \tan\alpha$. For values of α used in most rail systems, the ratio $\left(L/V\right) = \tan\alpha$ is much larger than one, implying that Nadal's formula suggests lubrication significantly increases the L/V limit. The quasi-static analysis can lead to contradictory results as in case of predominantly longitudinal friction force. Such concerns can be further explained using spatial dynamic analysis to account for the inertia-force effect on the normal force N that enters into formulating the friction force μN.

2. SCOPE AND CONTRIBUTIONS OF THIS STUDY

Despite limitations addressed in the literature [3], a large number of investigations have been devoted to developing and validating $\left(L/V\right)$-based derailment criteria [4 – 9]; examples of which are Nadal single-wheel L/V limit criterion, Weinstock axle-sum L/V limit criterion, FRA high speed passenger distance limit (5 ft), AAR Chapter 11 50-millisecond time limit, Japanese National Railway (JNR) L/V time duration criterion, EMD L/V time duration criterion, and TTCI wheel climb distance criterion. In Weinstock's criterion [10], two wheels instead of single wheel and non-flange-wheel friction are considered. The derailment is predicted by summing absolute values of the L/V ratios of two wheels rigidly connected by an axle; the sum is known as the *axle sum* L/V *ratio*. The JNR and EMD time-duration criteria suggest increasing the L/V

limit if lateral-thrust duration is less than certain time duration; with the JNR criterion assuming time duration of 50 ms [11], while the EMD is considered less conservative [12]. The AAR wheel climb-duration limit proposes using 50 ms (0.05 s); while the FRA wheel-climb distance limit proposes 5 ft limit for class 6 and higher in case of high speed rails. The TTCI wheel climb distance criterion, developed for freight trains with AAR1B wheel profile and $75°$ flange angle, considers both Nadal's L/V limit and the L/V distance limit that do not account for the angle of attack, is considered applicable for speeds below 80 km/h in case of curving. Studies on effect of flange angle ranging from $63°$ to $75°$ on the L/V ratio show that increasing the flange length can lead to increasing flange climb-distance limit, particularly in case of small angle of attack [8, 9].

2.1 Scope and Contributions of the Study

The scope and contributions of this investigations can be summarized as follows:

1. A new three-dimensional dynamic formulation is used to develop simple L/V ratio and incorporate the longitudinal component of the friction force using basic assumptions employed in deriving Nadal's ratio. A special case of the spatial dynamic analysis confirms results previously obtained in the literature using a quasi-static intuitive engineering approach [6]. While the L/V formula obtained as a special case of the spatial dynamic formulation appears intuitive, the mathematical derivation confirms its correctness and demonstrates the dependence of the normal-reaction force on quadratic-velocity inertia forces.
2. A planar dynamic model is developed to demonstrate that Nadal's L/V limit corresponds to zero *climb acceleration* or quasi-static force analysis [13]. The zero climb-acceleration condition can be associated with flange downward motion since the velocity and acceleration signs can be different. Concept of *non-generalized coordinates* is used to develop planar dynamic model, define wheel-climb kinematic constraints, and determine constraint-reaction

force [14, 15]. It is shown that the absolute wheel acceleration is zero for the planar model when the climb component of the acceleration is zero.

3. Concept of non-generalized coordinates is used to develop new three-dimensional wheel-climb dynamic formulation, which accounts for the track curvature, super-elevation, and centrifugal and inertia forces that enter into definition of constraint-reaction forces. It is shown that the L/V ratio does not depend on the bank angle that defines the track super-elevation. The spatial dynamic formulation leads to an L/V ratio that demonstrates limitations of the planar static-force analysis. The spatial single-degree-of-freedom model developed can be used to define an *inverse problem* to study different climb patterns. It is shown that wheel acceleration can be zero for non-zero climb acceleration due to centrifugal and Coriolis acceleration components. Condition of zero wheel acceleration and non-zero climb acceleration is formulated. Based on the analysis presented in this study, a new approach that can be used to define the wheel-climb pattern based on simple experimental measurements is introduced.
4. Effect of the longitudinal component of the friction force on the L/V ratio is demonstrated. This friction-force component is not accounted for in the planar analysis. The fact that the longitudinal friction-force component can significantly alter magnitude of the L/V ratio demonstrates the need for accurate measurement of the climb velocity to have an accurate estimate of the L/V ratio. It is demonstrated that by properly accounting for friction-force direction using the spatial analysis, the L/V limit can approach four, justifying concerns regarding the limits currently used in accident investigations.

2.2 Friction-Force Direction and Pitch Rotation

In deriving Nadal's limit, it is assumed that the friction force in its totality acts upward due to the wheel rotation, which is not considered in the mathematical derivation of the L/V ratio.

Furthermore, the sliding down of the wheel contact point on the rail due to the wheel *pitch rotation* in case of large angle of attack does not imply that direction of the relative velocity is downward; the cross product of the wheel angular velocity and local position vector of the contact point can define a vector which is predominantly longitudinal. In the spatial dynamic formulation used in this study, it is assumed that the friction force is opposite to the direction of the relative velocity between the wheel and rail. Nonetheless, there are obvious concerns regarding the use of orientation of the friction force in deriving Nadal's formula [3]: (1) In case of flange contact at zero or small angle of attack, the contact point shifts closer to the wheel center in the longitudinal direction and the direction of the friction force becomes predominantly longitudinal. That is, in general, one cannot in general assume that the friction force is in the direction used in deriving Nadal's limit [3, 6]; (2) During wheel climb and as the result of the tread contact of the other wheel, the wheel continues to move forward with a significant longitudinal relative velocity component that has an influence on the direction of the friction force and such a component cannot be ignored. Furthermore, the absolute velocity of the contact point on the wheel is the sum of two components: the velocity of the wheel reference point $\dot{\mathbf{R}}^w$ and the velocity of the contact point with respect to the reference point due to the wheel rotation. The reference-point velocity can be influenced by the suspension forces and roll moment resulting from the non-flange contact at the other wheel. Therefore, assuming that the friction force in its totality is along the flange cannot be justified and it is doubtful that such scenario dominates wheel-climb mechanics; and (3) Nadal's planar force analysis does not account for the wheel rotation or angle of attack. In such an analysis, the proper mathematical treatment is based on assuming the climb is associated with upward relative velocity (since pitch rotation is not considered). Furthermore, the quasi-static force balance

used can be applicable to wheel climb as well as when the wheel sliding down, and therefore, such a force analysis is not indicative of or particular to wheel climb.

2.3 Positive-Train-Control (PTC) Algorithms

While this study proposes a new procedure for developing an L/V ratio based on spatial dynamic analysis, no recommendations are made regarding derailment and no derailment criterion is developed. Furthermore, this study does not suggest that increasing the lateral force does not contribute to increasing the possibility of wheel climb. Credible derailment and wheel-climb criteria require extensive analytical and numerical investigations that are not within the scope of this investigation. Nonetheless, the proposed approach can be used as the basis for developing real-time *positive-train-control* (PTC) algorithms, implemented on onboard computers, to define wheel-climb pattern using online measurements. Such PTC algorithms can produce, in real-time, results that define the climb acceleration, velocity, and displacement. Such online information, if properly used with control actions, can contribute to avoiding wheel-climb derailments during curve negotiations.

3. PLANAR WHEEL-CLIMB KINEMATICS

The assumptions used in developing Nadal's L/V ratio based on quasi-static considerations are followed in this study to develop a planar wheel-climb dynamic model that sheds light on the effect of the lateral and vertical forces on the direction of the acceleration along wheel flange. However, before developing such simplified wheel-climb model, a more general kinematic approach is described in this section to highlight simplifications which allow using Newton equations only instead of Newton-Euler equations for describing the wheel motion.

In case of planar analysis, vectors tangent and normal to the flange, shown in Fig. 1, can be defined in a wheel coordinate system, respectively, as

$$\bar{\mathbf{t}}^w = \begin{bmatrix} \cos\alpha & \sin\alpha \end{bmatrix}^T, \quad \bar{\mathbf{n}}^w = \begin{bmatrix} -\sin\alpha & \cos\alpha \end{bmatrix}^T \tag{1}$$

where α is the flange angle. Wheel motion can be described using three coordinates; two coordinates $\mathbf{R}^w = \begin{bmatrix} R_1^w & R_2^w \end{bmatrix}^T$ describe translation of wheel center of mass, and one angle θ^w defines wheel angular orientation. If sliding along the flange is considered as the only degree of freedom as it is the case when deriving Nadal's L/V ratio, the wheel is subjected to two motion constraints; one of the constraints eliminates the rotational displacement during the climb, that is, $\theta^w = c_r$ where c_r is a constant. If the non-generalized coordinate (surface parameter) s^w is introduced to describe the wheel climb, two additional motion constraints are required to define single-degree-of-freedom wheel-climb model. The location of the contact point on the wheel flange can be written in terms of the non-generalized coordinate s^w as $\mathbf{r}^w = \mathbf{R}^w + \mathbf{A}^w \bar{\mathbf{u}}_c^w = \mathbf{R}^w + \mathbf{A}^w \left(\bar{\mathbf{u}}_o^w + s^w \bar{\mathbf{t}}^w \right)$, where $\mathbf{A}^w$ is the planar transformation matrix that defines the wheel orientation, $\bar{\mathbf{u}}_c^w = \bar{\mathbf{u}}_o^w + s^w \bar{\mathbf{t}}^w$ is the contact-point position vector with respect to the wheel coordinate system, $\bar{\mathbf{u}}_o^w$ is a constant vector that defines the lateral position of the point on the wheel, and $\mathbf{t}^w = \mathbf{A}^w \bar{\mathbf{t}}^w$ [15]. Assuming fixed contact point on the rail during the climb, one can write the constraint equations $\mathbf{r}^{wr} = \mathbf{R}^w + \mathbf{A}^w \bar{\mathbf{u}}_c^w - \mathbf{R}^r = \mathbf{0}$, where in the planar analysis $\mathbf{R}^r$ is constant vector that defines the location of the contact point on the rail.

Following the assumptions used in deriving Nadal's limit, assuming $\theta^w = c_r = 0$, which eliminates the rotational degree of freedom and the associated Euler equation of motion and leads to an identity rotation matrix, that is, $\mathbf{A}^w = \mathbf{I}$, one has $\mathbf{t}^w = \mathbf{A}^w \bar{\mathbf{t}}^w = \bar{\mathbf{t}}^w$ and the planar wheel motion

is subjected to the following two kinematic constraints written in terms of three generalized and non-generalized coordinates $\mathbf{p} = \begin{bmatrix} \mathbf{R}^{w^T} & s^w \end{bmatrix}^T$:

$$\mathbf{r}^{wr} = \mathbf{R}^w + \left(\overline{\mathbf{u}}_o^w + s^w \overline{\mathbf{t}}^w \right) - \mathbf{R}^r = \mathbf{0} \tag{2}$$

This equation shows that

$$\left.\begin{aligned} s^w &= \overline{\mathbf{t}}^{w^T} \left(\mathbf{R}^r - \mathbf{R}^w - \overline{\mathbf{u}}_o^w \right), \\ \ddot{s}^w &= -\overline{\mathbf{t}}^{w^T} \ddot{\mathbf{R}}^w, \quad \ddot{\mathbf{R}}^w = -\ddot{s}^w \overline{\mathbf{t}}^w \end{aligned}\right\} \tag{3}$$

Alternatively, the non-generalized coordinate s^w can be eliminated leading to only one constraint equation that can be combined with the two equations of motion to define a one-degree-of-freedom model. For example, pre-multiplying $\ddot{\mathbf{R}}^w = -\ddot{s}^w \overline{\mathbf{t}}^w$ by $\mathbf{n}^{w^T}$ and using $\mathbf{n}^w = \mathbf{A}^w \overline{\mathbf{n}}^w$ and $\mathbf{A}^w = \mathbf{I}$, one has single constraint equation at the acceleration level $\ddot{C} = \mathbf{n}^{w^T} \ddot{\mathbf{R}}^w = -\ddot{R}_1^w \sin\alpha + \ddot{R}_2^w \cos\alpha = 0$. It is clear from $\ddot{\mathbf{R}}^w = -\ddot{s}^w \overline{\mathbf{t}}^w$ that in case of Nadal's planar model, the wheel absolute acceleration $\ddot{\mathbf{R}}^w$ is zero if the climb acceleration $\ddot{s}^w$ is zero. As will be shown, this is not the case when the spatial analysis is considered.

4. PLANAR CLIMB DYNAMIC EQUATIONS

Because wheel rotation can be eliminated, planar wheel-climb dynamics is governed by two Newton equations subject to the constraint equation C. The equations of motion and the constraint equation at the acceleration level can be written as

$$\left.\begin{aligned} \mathbf{M}^w \ddot{\mathbf{R}}^w &= \mathbf{F}^w + \mathbf{F}_c^w, \\ \ddot{C} &= \mathbf{n}^{w^T} \ddot{\mathbf{R}}^w = -\ddot{R}_1^w \sin\alpha + \ddot{R}_2^w \cos\alpha = 0 \end{aligned}\right\} \tag{4}$$

where $\mathbf{M}^w = m^w\mathbf{I}, \mathbf{F}^w = \begin{bmatrix} F_1^w & F_2^w \end{bmatrix}^T, \mathbf{F}_c^w = -C_{\mathbf{R}^w}^T\lambda = -\mathbf{n}^w\lambda$, m^w is wheel mass, $\mathbf{F}^w$ is vector of applied forces, $\mathbf{F}_c^w$ is vector of constraint force, $C_{\mathbf{R}^w} = \partial C/\partial \mathbf{R}^w$ is constraint Jacobian matrix, and λ is Lagrange multiplier which, in this case, equals the reaction force N normal to the contact surface. That is, $\lambda = N$ [15]. The equations of motion and constraint equation at the acceleration level can be written in the augmented Lagrangian form as

$$\begin{bmatrix} m^w & 0 & -\sin\alpha \\ 0 & m^w & \cos\alpha \\ -\sin\alpha & \cos\alpha & 0 \end{bmatrix} \begin{bmatrix} \ddot{R}_1^w \\ \ddot{R}_2^w \\ \lambda \end{bmatrix} = \begin{bmatrix} F_1^w \\ F_2^w \\ 0 \end{bmatrix} \tag{5}$$

The solution of this equation defines the accelerations and Lagrange multiplier in terms of $\mathbf{F}^w$ as

$$\left.\begin{aligned} \ddot{\mathbf{R}}^w &= \begin{bmatrix} \ddot{R}_1^w & \ddot{R}_2^w \end{bmatrix}^T = \left(1/m^w\right)\left[\mathbf{F}^w - \left(\mathbf{n}^{w^T}\mathbf{F}^w\right)\mathbf{n}^w\right] \\ \lambda &= N = \mathbf{n}^{w^T}\mathbf{F}^w = -F_1^w\sin\alpha + F_2^w\cos\alpha \end{aligned}\right\} \tag{6}$$

This solution can be verified by pre-multiplying the equation of motion by the transpose of the normal vector $\mathbf{n}^w$ to obtain $\mathbf{n}^{w^T}\mathbf{M}^w\ddot{\mathbf{R}}^w = \mathbf{n}^{w^T}\left(\mathbf{F}^w + \mathbf{F}_c^w\right)$. Since $\mathbf{M}^w = m^w\mathbf{I}$ and the acceleration component along the normal vector must be zero because of the climb constraints, one has $\mathbf{n}^{w^T}\mathbf{F}_c^w = \mathbf{n}^{w^T}\left(-\mathbf{n}^w\lambda\right) = -\mathbf{n}^{w^T}\mathbf{F}^w$, defining Lagrange multiplier as $\lambda = N = \mathbf{n}^{w^T}\mathbf{F}^w$, which when substituted into the equation of motion leads to $\ddot{\mathbf{R}}^w = \left(1/m^w\right)\left(\mathbf{F}^w - \mathbf{n}^w\left(\mathbf{n}^{w^T}\mathbf{F}^w\right)\right)$, verifying the solution previously obtained. The acceleration vector $\ddot{\mathbf{R}}^w$ can also be written as $\ddot{\mathbf{R}}^w = \left(1/m^w\right)\mathbf{P}_{pn}^w\mathbf{F}^w$, where $\mathbf{P}_{pn}^w = \mathbf{I} - \mathbf{n}^w \otimes \mathbf{n}^w = \mathbf{I} - \mathbf{n}^w\mathbf{n}^{w^T}$ is a *projection matrix* and $\mathbf{n}^w \otimes \mathbf{n}^w = \mathbf{n}^w\mathbf{n}^{w^T}$ is the outer (dyadic) product. It can be shown that $\mathbf{P}_{pn}^w\mathbf{n}^w = \mathbf{0}$ and $\mathbf{n}^{w^T}\mathbf{P}_{pn}^w = \mathbf{0}^T$.

5. WHEEL-CLIMB ANALYSIS

Planar wheel-climb analysis of the preceding section shows that the acceleration vector can be written in terms of the applied forces as $\ddot{\mathbf{R}}^w = \left(1/m^w\right)\left(\mathbf{F}^w - \mathbf{n}^w\left(\mathbf{n}^{w^T}\mathbf{F}^w\right)\right)$. This acceleration vector has zero component along the normal to the wheel/rail contact surface, that is, $\mathbf{n}^{w^T}\ddot{\mathbf{R}}^W = 0$.

5.1 Climb Acceleration

The projection of the acceleration vector along the tangent to the wheel flange defines the *climb acceleration*, which can be written as

$$\begin{aligned}\mathbf{t}^{w^T}\ddot{\mathbf{R}}^w &= \left(1/m^w\right)\mathbf{t}^{w^T}\left(\mathbf{F}^w - \mathbf{n}^w\left(\mathbf{n}^{w^T}\mathbf{F}^w\right)\right)\\ &= \left(1/m^w\right)\mathbf{t}^{w^T}\mathbf{F}^w = \left(1/m^w\right)\left(F_1^w\cos\alpha + F_2^w\sin\alpha\right)\end{aligned} \tag{7}$$

At time of zero tangential acceleration, one has $\mathbf{t}^{w^T}\mathbf{F}^w = \left(F_1^w\cos\alpha + F_2^w\sin\alpha\right) = 0$. That is, at the point of instantaneous zero acceleration or in case of quasi-static analysis, regardless of the magnitude of the reaction force N, one has $F_1^w/F_2^w = -\sin\alpha/\cos\alpha$.

5.2 Nadal's Lateral and Vertical Forces

In Nadal's planar force balance, the lateral and vertical forces L and V, respectively, are defined as the resultant of all applied forces excluding the friction force μN. In case of wheel climb, the friction force $\mathbf{F}_f^w$ acts downward along the flange slope. That is, $\mathbf{F}_f^w = -F\mathbf{t}^w = -\left(\mu N\right)\mathbf{t}^w$, where $F = \mu N$. In this case, Nadal definition of the lateral ad vertical force is

$$\begin{bmatrix} L & -V\end{bmatrix}^T = \mathbf{F}^w - \left(\mu N\right)\mathbf{t}^w \tag{8}$$

In developing Nadal's L/V ratio, it is assumed that the friction force acts upward due to the wheel rotation and the angle of attack α_a. In this case, and to keep the same assumptions used in

developing Nadal's L/V ratio, the preceding equation is altered to $\begin{bmatrix} L & -V \end{bmatrix}^T = \mathbf{F}^w + (\mu N)\mathbf{t}^w$. As previously discussed, there are concerns regarding the use of positive direction of the friction force that include validity of this assumption in case of flange contact at zero angle of attack; change in direction of the velocity component of the wheel due to rotation and direction of the friction force as the climb displacement increases and the contact point shifts closer to the wheel center in the longitudinal direction; the wheel forward-velocity and friction-force components in the longitudinal direction can be significant and cannot be ignored; absolute velocity of the contact point is the sum of two components and is not only the result of the wheel rotation; and Nadal's planar force analysis does not account for the wheel rotation or angle of attack [3]. Despite these concerns, the equation $\begin{bmatrix} L & -V \end{bmatrix}^T = \mathbf{F}^w + (\mu N)\mathbf{t}^w$ is used to write $\mathbf{t}^{w^T}\ddot{\mathbf{R}}^w = (1/m^w)\mathbf{t}^{w^T}\mathbf{F}^w$ as

$$\mathbf{t}^{w^T}\ddot{\mathbf{R}}^w = (1/m^w)\mathbf{t}^{w^T}\mathbf{F}^w = (1/m^w)(L\cos\alpha - V\sin\alpha - \mu N) \tag{9}$$

Since $N = \lambda = \mathbf{n}^{w^T}\mathbf{F}^w$, one has

$$\begin{aligned} N = \mathbf{n}^{w^T}\mathbf{F}^w &= \mathbf{n}^{w^T}\left(\begin{bmatrix} L & -V \end{bmatrix}^T + \mu N\mathbf{t}^w\right) \\ &= \mathbf{n}^{w^T}\begin{bmatrix} L & -V \end{bmatrix}^T = -L\sin\alpha - V\cos\alpha \end{aligned} \tag{10}$$

Therefore,

$$\begin{aligned} \mathbf{t}^{w^T}\ddot{\mathbf{R}}^w &= (1/m^w)\mathbf{t}^{w^T}\mathbf{F}^w \\ &= (1/m^w)\left(L(\cos\alpha + \mu\sin\alpha) - V(\sin\alpha - \mu\cos\alpha)\right) \\ &= (1/m^w)(c_L L + c_V V) \end{aligned} \tag{11}$$

where $c_L = \cos\alpha + \mu\sin\alpha$ and $c_V = \sin\alpha - \mu\cos\alpha$. At points of instantaneous zero climb acceleration or in case of quasi-static analysis, $\mathbf{t}^{w^T}\ddot{\mathbf{R}}^w = 0$, and one has $L(\cos\alpha + \mu\sin\alpha) - V(\sin\alpha - \mu\cos\alpha) = 0$, which leads to Nadal's limit

$$\frac{L}{V}=\frac{\sin\alpha-\mu\cos\alpha}{\cos\alpha+\mu\sin\alpha}=\frac{\tan\alpha-\mu}{1+\mu\tan\alpha} \tag{12}$$

This equation demonstrates that the simple wheel-climb dynamic analysis leads to Nadal's limit if the climb acceleration is zero, that is, $\mathbf{t}^{w^T}\ddot{\mathbf{R}}^w=0$. In case of flange angle $\alpha=72°$ and coefficient of friction $\mu=0.5$, Nadal's limit is $L/V=1.0153$. In this case, the coefficient of L and V in the tangential equation of motion are, respectively, $c_L=0.7845$ and $c_V=0.7965$.

5.3 Nadal's Limit and Three-Dimensional Analysis

In addition to using planar analysis only when deriving Nadal's L/V ratio, an assumption is made that the friction force in its totality acts opposite to the wheel climb. There are, however, two modes of sliding. The first mode is sliding in the direction of the forward motion, which is not characterized by a pure rolling, while the second sliding mode is the climb of the wheel. These two sliding modes define friction-force components in case of wheel climb, which can occur at low speed relative to the forward velocity of the wheel.

The friction force in its totality acts in a direction opposite to the direction of the relative velocity between the wheel and the rail. In case of wheel climb, it is assumed that the wheel flange maintains contact with the rail inner surface, and the relative velocity between the wheel and rail can have the above-described two components; a component in the climb direction and the other in the forward-motion direction; both components oppose the motion. The forward-velocity component is proportional to the magnitude of the wheel angular velocity $\boldsymbol{\omega}^w$ and the radial location of the contact point defined by the vector $\mathbf{r}_c^w$, that is, the forward velocity at the contact point due to the sliding velocity v_f^w in the forward direction is approximately equal to $\left|\boldsymbol{\omega}^w\times\mathbf{r}_c^w\right|$. Since the climb velocity v_c^w can be small compared to the forward velocity v_f^w during the climb,

that is, $\left|v_c^w / v_f^w\right| \ll 1$, the friction force can be predominantly longitudinal making the friction force that opposes the climb small in comparison to the normal reaction force N. In this case, Nadal's limit based on the planar analysis can be written as $L/V \approx \tan\alpha$. This limit for a flange angle of 75^0 is approximately 3.73. Furthermore, in practical motion scenarios, the vibration of the track due to the rail flexibility and foundation movements can have significant effect on the direction of the wheel/rail relative velocity, and for this reason, performing computer simulations based on fully nonlinear models may be required to identify root causes of accidents.

6. SPATIAL KINEMATICS

While wheelset rotations and moments cannot, in general be ignored in the analysis of wheel/rail interaction forces, a simplified three-dimensional dynamic model consistent with Nadal's assumptions can still be developed to examine the effect of the forward motion and develop a simple model that can be used to define the climb pattern and develop a real-time PTC algorithm.

6.1 Wheel Kinematics

In this study, motion constraints are applied to obtain single-degree-of-freedom wheel-climb model that accounts for the forward motion on a curve. To this end, the flange geometry is defined in the wheel coordinate system by the following tangent and normal vectors, respectively:

$$\bar{\mathbf{t}}^w = \begin{bmatrix} 0 & -\cos\alpha & \sin\alpha \end{bmatrix}^T, \quad \bar{\mathbf{n}}^w = \begin{bmatrix} 0 & \sin\alpha & \cos\alpha \end{bmatrix}^T \tag{13}$$

These vectors are defined with the assumption that X_1 is the longitudinal axis in the motion direction, X_2 is the lateral axis, and X_3 is the vertical axis.

The wheel orientation can be described using the three Euler angles ψ, ϕ, and θ about the wheel X_3, X_1, and X_2 axes, respectively [15]. In the three-dimensional model developed in this

study, the roll angle ϕ and pitch angle θ are constrained, while the yaw angle ψ is defined as $\psi = s^r / R^r$ where s^r is the curve arc length and R^r is the curve radius of curvature [15]. The yaw angle ψ is assumed to account for the angle of attack α_a. The position of an arbitrary point on the wheel flange can be written as $\mathbf{r}^w = \mathbf{R}^w + \mathbf{A}^w\left(\bar{\mathbf{u}}_o^w + s^w \bar{\mathbf{t}}^w\right)$, where $\bar{\mathbf{u}}_o^w$ and s^w are, respectively, lateral position vector and surface parameter that defines contact-point location, and

$$\mathbf{A}^w = \begin{bmatrix} \cos\psi & -\sin\psi & 0 \\ \sin\psi & \cos\psi & 0 \\ 0 & 0 & 1 \end{bmatrix}, \quad \mathbf{t}^w = \mathbf{A}^w \bar{\mathbf{t}}^w = \begin{bmatrix} \cos\alpha\sin\psi \\ -\cos\alpha\cos\psi \\ \sin\alpha \end{bmatrix}, \quad \mathbf{n}^w = \mathbf{A}^w \bar{\mathbf{n}}^w = \begin{bmatrix} -\sin\alpha\sin\psi \\ \sin\alpha\cos\psi \\ \cos\alpha \end{bmatrix} \tag{14}$$

Assuming constant forward velocity, one has $\dot{\psi} = \dot{s}^r / R^r$. One also has the following identities and derivatives, where $\mathbf{A}_\psi^w = \partial \mathbf{A}^w / \partial \psi$:

$$\left.\begin{aligned} &\mathbf{A}^{wT}\mathbf{A}_\psi^w = \tilde{\mathbf{I}} = \begin{bmatrix} 0 & -1 & 0 \\ 1 & 0 & 0 \\ 0 & 0 & 0 \end{bmatrix}, \quad \mathbf{A}_{\psi\psi}^w = \partial^2 \mathbf{A}^w / \partial \psi^2 = -\begin{bmatrix} \cos\psi & -\sin\psi & 0 \\ \sin\psi & \cos\psi & 0 \\ 0 & 0 & 0 \end{bmatrix} = -\mathbf{A}_{sd}^w \\ &\dot{\mathbf{t}}^w = \dot{\psi}\mathbf{A}_\psi^w \bar{\mathbf{t}}^w = \dot{\psi}\begin{bmatrix} \cos\alpha\cos\psi \\ \cos\alpha\sin\psi \\ 0 \end{bmatrix}, \quad \dot{\mathbf{n}}^w = \dot{\psi}\mathbf{A}_\psi^w \bar{\mathbf{n}}^w = \dot{\psi}\begin{bmatrix} -\sin\alpha\cos\psi \\ -\sin\alpha\sin\psi \\ 0 \end{bmatrix}, \\ &\ddot{\mathbf{t}}^w = -\left(\dot{\psi}\right)^2 \mathbf{A}_{sd}^w \bar{\mathbf{t}}^w = -\left(\dot{\psi}\right)^2 \begin{bmatrix} \cos\alpha\sin\psi \\ -\cos\alpha\cos\psi \\ 0 \end{bmatrix}, \quad \ddot{\mathbf{n}}^w = -\left(\dot{\psi}\right)^2 \mathbf{A}_{sd}^w \bar{\mathbf{n}}^w = -\left(\dot{\psi}\right)^2 \begin{bmatrix} -\sin\alpha\sin\psi \\ \sin\alpha\cos\psi \\ 0 \end{bmatrix} \end{aligned}\right\} \tag{15}$$

To describe wheel/rail contact, two surface parameters are used: the first is the wheel surface parameter s^w used to define contact-point location, and the second is the rail surface parameter s^r which defines the distance travelled by the wheel [15, 16]. A contact frame can be defined on the wheel surface by three orthogonal unit vectors $\mathbf{t}_l^w, \mathbf{n}^w$, and $\mathbf{t}^w$, where $\mathbf{t}_l^w = \mathbf{n}^w \times \mathbf{t}^w = \begin{bmatrix} \cos\psi & \sin\psi & 0 \end{bmatrix}^T$. Using surface parameter s^w, the global position vector of the

contact point on the wheel can be written, as previously discussed, as $\mathbf{r}^w = \mathbf{R}^w + \mathbf{A}^w \bar{\mathbf{u}}_o^w + s^w \mathbf{t}^w$, where $\mathbf{R}^w = \begin{bmatrix} R_1^w & R_2^w & R_3^w \end{bmatrix}^T$ is the global position vector of the wheel mass center.

6.2 Rail Geometry

The location of an arbitrary point on the rail can be written in case of a curve with zero super-elevation in terms of the rail surface parameter s^r as $\mathbf{R}^r\left(s^r\right) = R^r \begin{bmatrix} \sin\psi & -\cos\psi & 0 \end{bmatrix}^T$. The unit tangent to the rail at a potential contact point is defined as $\mathbf{t}^r = \begin{bmatrix} \cos\psi & \sin\psi & 0 \end{bmatrix}^T = \mathbf{t}_l^w$. Using these definition, one has

$$\left.\begin{aligned} \mathbf{A}_\psi^{w^T} \mathbf{R}^r &= -R^r \mathbf{i} = -R^r \begin{bmatrix} 1 & 0 & 0 \end{bmatrix}^T, \\ \mathbf{A}^{w^T} \mathbf{t}^r &= \mathbf{i} = \begin{bmatrix} 1 & 0 & 0 \end{bmatrix}^T \end{aligned}\right\} \tag{16}$$

That is, $\mathbf{t}^r = \begin{bmatrix} \cos\psi & \sin\psi & 0 \end{bmatrix}^T = \mathbf{t}_l^w$ remains along the wheel longitudinal axis. In case of non-zero super-elevation by a bank angle ϕ^r performed about the $-X_1$ axis,

$$\left.\begin{aligned} \mathbf{R}^r\left(s^r\right) &= R^r \begin{bmatrix} \sin\psi & -\cos\psi\cos\phi^r & \cos\psi\sin\phi^r \end{bmatrix}^T \\ \mathbf{t}^r &= \begin{bmatrix} \cos\psi & \sin\psi\cos\phi^r & -\sin\psi\sin\phi^r \end{bmatrix}^T \end{aligned}\right\} \tag{17}$$

In case of constant $\dot{\psi}$, the preceding equation shows that $\dot{\mathbf{R}}^r = \dot{\psi} R^r \mathbf{t}^r$, $\ddot{\mathbf{R}}^r = -\left(\dot{\psi}\right)^2 \mathbf{R}^r$, and $\mathbf{t}^{r^T} \mathbf{t}_l^w = \cos^2\psi + \sin^2\psi\cos\phi^r$, which shows the effect of the bank angle. If the bank angle ϕ^r is small, $\cos\phi^r \approx 1$ and $\mathbf{t}^{r^T} \mathbf{t}_l^w \approx 1$.

7. SPATIAL MOTION CONSTRAINTS

To obtain single-degree-of-freedom wheel-climb model based on the three spatial Newton equations of motion, four kinematic constraints are applied since two surface parameters s^w and s^r are introduced. These four constraint equations are

$$\left.\begin{aligned} \mathbf{r}^{wr} &= \mathbf{r}^w - \mathbf{R}^r = \mathbf{R}^w + \mathbf{A}^w\bar{\mathbf{u}}_o^w + s^w\mathbf{t}^w - \mathbf{R}^r = \mathbf{0} \\ s^r - v^w t &= 0 \end{aligned}\right\} \tag{18}$$

where v^w is the forward velocity of the flange contact point which is assumed constant. The fourth equation in the preceding equation can be used to eliminate s^r as an unknown from the first three equations, that is, $\mathbf{R}^r$ becomes known function of time. This reduces the number of constraint equations to three equations, which can be written as

$$\mathbf{C} = \begin{bmatrix} C_1 & C_2 & C_3 \end{bmatrix}^T = \mathbf{R}^w + \mathbf{A}^w\bar{\mathbf{u}}_o^w + s^w\mathbf{t}^w - \mathbf{R}^r = \mathbf{0} \tag{19}$$

Pre-multiplying these equations by $\mathbf{t}^{w^T}$ and denoting $\mathbf{u}_o^w = \mathbf{A}^w\bar{\mathbf{u}}_o^w$ lead to

$$s^w = -\mathbf{t}^{w^T}\left(\mathbf{R}^w + \mathbf{u}_o^w - \mathbf{R}^r\right) \tag{20}$$

This equation can be used to eliminate s^w and reduce number of constraint equations to two. The constraint equations $\mathbf{C}$ lead to the following velocity and acceleration equations assuming that $\dot{s}^r$, or equivalently $\dot{\psi}$, is constant:

$$\left.\begin{aligned} \dot{\mathbf{R}}^w &= -\dot{\psi}\mathbf{A}_\psi^w\bar{\mathbf{u}}_c^w + \dot{\psi}R^r\mathbf{t}^r - \dot{s}^w\mathbf{t}^w \\ \ddot{\mathbf{R}}^w &= \left(\dot{\psi}\right)^2\left[\mathbf{A}_{sd}^w\bar{\mathbf{u}}_c^w - \mathbf{R}^r\right] - 2\dot{s}^w\dot{\psi}\mathbf{A}_\psi^w\bar{\mathbf{t}}^w - \ddot{s}^w\mathbf{t}^w \\ &= -\ddot{s}^w\mathbf{t}^w + \bar{\boldsymbol{\gamma}}^w \end{aligned}\right\} \tag{21}$$

where $\bar{\mathbf{u}}_c^w = \bar{\mathbf{u}}_o^w + s^w\bar{\mathbf{t}}^w$, $\bar{\boldsymbol{\gamma}}^w = \left(\dot{\psi}\right)^2\left[\mathbf{A}_{sd}^w\bar{\mathbf{u}}_c^w - \mathbf{R}^r\right] - 2\dot{s}^w\dot{\psi}\mathbf{A}_\psi^w\bar{\mathbf{t}}^w$, and $\mathbf{u}_c^w = \mathbf{A}^w\bar{\mathbf{u}}_c^w$. The preceding equation represents the constraint equations at the velocity and acceleration levels. The acceleration equation contains centrifugal and Coriolis acceleration terms. The equation

$\ddot{\mathbf{R}}^w = -\ddot{s}^w \mathbf{t}^w + \overline{\boldsymbol{\gamma}}^w$ shows that zero climb acceleration, $\ddot{s}^w = 0$, does not imply $\ddot{\mathbf{R}}^w = \mathbf{0}$ due to the curving behavior; and if $\ddot{s}^w = 0$, one has $\ddot{\mathbf{R}}^w = \overline{\boldsymbol{\gamma}}^w$. Using the definition $s^w = -\mathbf{t}^{w^T}\left(\mathbf{R}^w + \mathbf{u}_o^w - \mathbf{R}^r\right)$, the following velocity and acceleration equations can be developed:

$$\left.\begin{aligned} \dot{s}^w &= -\mathbf{t}^{w^T}\left(\dot{\mathbf{R}}^w + \dot{\psi}\mathbf{A}_\psi^w \overline{\mathbf{u}}_o^w - \dot{\mathbf{R}}^r\right) - \dot{\mathbf{t}}^{w^T}\left(\mathbf{R}^w + \mathbf{u}_o^w - \mathbf{R}^r\right) \\ &= -\mathbf{t}^{w^T}\dot{\mathbf{R}}^w + \gamma_s \\ \ddot{s}^w &= -\mathbf{t}^{w^T}\ddot{\mathbf{R}}^w + \left(\dot{\psi}\right)^2 \mathbf{t}^{w^T}\left[\mathbf{A}_{sd}^w \overline{\mathbf{u}}_c^w - \mathbf{R}^r\right] \end{aligned}\right\} \tag{22}$$

where $\gamma_s = -\mathbf{t}^{w^T}\left(\dot{\psi}\mathbf{A}_\psi^w \overline{\mathbf{u}}_o^w - \dot{\mathbf{R}}^r\right) - \dot{\psi}\overline{\mathbf{t}}^{w^T}\mathbf{A}_\psi^w\left(\mathbf{R}^w + \mathbf{u}_o^w - \mathbf{R}^r\right)$.

The equation $\ddot{\mathbf{R}}^w = -\ddot{s}^w \mathbf{t}^w + \overline{\boldsymbol{\gamma}}^w$ can play an important in defining the climb pattern in accident investigations. If the vector $\ddot{\mathbf{R}}^w$ can be measured, the climb acceleration $\ddot{s}^w$ can be determined from the equation $\ddot{s}^w = \mathbf{t}^{w^T}\left(-\ddot{\mathbf{R}}^w + \left(\dot{\psi}\right)^2\left[\mathbf{A}_{sd}^w \overline{\mathbf{u}}_c^w - \mathbf{R}^r\right]\right)$ for a given forward velocity $\dot{s}^r$ and track geometry. This measured climb acceleration can be numerically integrated to determine $\dot{s}^w$ and s^w.

8. SPATIAL WHEEL-CLIMB DYNAMIC MODEL

To generalize Nadal's analysis and assess the effect of such a generalization on L/V definition, the spatial Newton equations $m^w \ddot{\mathbf{R}}^w = \mathbf{F}^w + \mathbf{F}_c^w$ are considered, where $\mathbf{F}^w$ and $\mathbf{F}_c^w$ are three-dimensional vectors that define, respectively, applied and constraint forces.

8.1 Single-Degree-of-Freedom Model and Inverse Problem

Substituting $\ddot{\mathbf{R}}^w$ defined in the preceding section into Newton equations, pre-multiplying by $\mathbf{t}^{w^T}$, and using $\mathbf{t}^{w^T}\mathbf{F}_c^w = 0$ because non-generalized coordinate s^w is treated as the degree of freedom, one obtains

$$m^w \ddot{s}^w = \mathbf{t}^{w^T}\left(-\mathbf{F}^w + m^w\left(\dot{\psi}\right)^2\left[\mathbf{A}_{sd}^w\bar{\mathbf{u}}_c^w - \mathbf{R}^r\right]\right) \tag{23}$$

This equation shows that

$$\begin{aligned}\ddot{s}^w &= \mathbf{t}^{w^T}\left(-\left(\mathbf{F}^w/m^w\right) + \left(\dot{\psi}\right)^2\left[\mathbf{A}_{sd}^w\bar{\mathbf{u}}_c^w - \mathbf{R}^r\right]\right)\\ &= -\left(\mathbf{t}^{w^T}\mathbf{F}^w/m^w\right) + \bar{\gamma}\end{aligned} \tag{24}$$

where $\bar{\gamma} = \left(\dot{\psi}\right)^2\mathbf{t}^{w^T}\left[\left(\mathbf{A}_{sd}^w\bar{\mathbf{u}}_o^w + s^w\right) - \mathbf{R}^r\right]$. The preceding equation, which shows the effect of the forward velocity on the climb acceleration, leads to

$$\ddot{\mathbf{R}}^w = -\ddot{s}^w\mathbf{t}^w + \bar{\boldsymbol{\gamma}}^w = \left(\mathbf{t}^{w^T}\mathbf{F}^w/m^w\right)\mathbf{t}^w + \left(\bar{\boldsymbol{\gamma}}^w - \bar{\gamma}\mathbf{t}^w\right) \tag{25}$$

Denoting $\boldsymbol{\gamma}^w = \bar{\boldsymbol{\gamma}}^w - \bar{\gamma}\mathbf{t}^w$, one has $\boldsymbol{\gamma}^w = \bar{\boldsymbol{\gamma}}^w - \bar{\gamma}\mathbf{t}^w = \bar{\boldsymbol{\gamma}}^w - \mathbf{t}^{w^T}\bar{\boldsymbol{\gamma}}^w\mathbf{t}^w = \mathbf{P}_p^w\bar{\boldsymbol{\gamma}}^w$, which can be written as, where $\mathbf{P}_p^w = \left(\mathbf{I} - \mathbf{t}^w \otimes \mathbf{t}^w\right)$ is a projection matrix that defines direction perpendicular to climb direction, and $\otimes$ refers to the dyadic or outer product. The accelerations can then be written as

$$\ddot{\mathbf{R}}^w = \left(1/m^w\right)\left(\mathbf{t}^{w^T}\mathbf{F}^w\right)\mathbf{t}^w + \boldsymbol{\gamma}^w \tag{26}$$

The constraint force vector $\mathbf{F}_c^w$ can then be defined as

$$\begin{aligned}\mathbf{F}_c^w &= m^w\ddot{\mathbf{R}}^w - \mathbf{F}^w = \left(\mathbf{t}^{w^T}\mathbf{F}^w\right)\mathbf{t}^w + m^w\boldsymbol{\gamma}^w - \mathbf{F}^w\\ &= \left[\left(\mathbf{t}^{w^T}\mathbf{F}^w\right)\mathbf{t}^w - \mathbf{F}^w\right] - m^w\left[\left(\mathbf{t}^{w^T}\bar{\boldsymbol{\gamma}}^w\right)\mathbf{t}^w - \bar{\boldsymbol{\gamma}}^w\right] = \left(\mathbf{t}^{w^T}\bar{\mathbf{F}}^w\right)\mathbf{t}^w - \bar{\mathbf{F}}^w\\ &= -\left(\mathbf{I} - \mathbf{t}^w \otimes \mathbf{t}^w\right)\bar{\mathbf{F}}^w = -\mathbf{P}_p^w\bar{\mathbf{F}}^w\end{aligned} \tag{27}$$

where $\overline{\mathbf{F}}^w = \mathbf{F}^w - m^w\overline{\boldsymbol{\gamma}}^w$. The preceding equation, upon substituting in $m^w\ddot{\mathbf{R}}^w = \mathbf{F}^w + \mathbf{F}_c^w$, eliminates constraint forces and leads to $m^w\ddot{\mathbf{R}}^w = \mathbf{F}^w - \mathbf{P}_p^w\left(\mathbf{F}^w - m^w\overline{\boldsymbol{\gamma}}^w\right)$, which can be written as $m^w\ddot{\mathbf{R}}^w = \mathbf{P}^w\mathbf{F}^w + m^w\mathbf{P}_p^w\overline{\boldsymbol{\gamma}}^w = \mathbf{F}_r^w$, where $\mathbf{F}_r^w = \mathbf{P}^w\mathbf{F}^w + m^w\mathbf{P}_p^w\overline{\boldsymbol{\gamma}}^w$ and $\mathbf{P}^w = \mathbf{t}^w \otimes \mathbf{t}^w$. The projection matrices $\mathbf{P}^w$ and $\mathbf{P}_p^w$ satisfy the identities $\mathbf{t}^{w^T}\mathbf{P}^w = \mathbf{t}^{w^T}$, $\mathbf{P}^w\mathbf{t}^w = \mathbf{t}^w$, $\mathbf{P}_p^w\mathbf{t}^w = \mathbf{0}$, and $\mathbf{t}^{w^T}\mathbf{P}_p^w = \mathbf{0}^T$.

8.2 Friction Force

Using the expression of $\mathbf{F}_c^w$, the normal reaction force is defined as

$$N = \mathbf{n}^{w^T}\mathbf{F}_c^w = \mathbf{n}^{w^T}\left[-\mathbf{P}_p^w\overline{\mathbf{F}}^w\right] = -\mathbf{n}^{w^T}\overline{\mathbf{F}}^w \tag{28}$$

In case of wheel climb, the ratio between the climb velocity v_c^w and forward wheel velocity $v_l^w = \dot{s}^w$ is $v_c^w / v_l^w = \tan\gamma_c$, which defines the friction force as

$$\mathbf{F}_f^w = -F\hat{\mathbf{v}}_c^w = -\mu N\hat{\mathbf{v}}_c^w \tag{29}$$

where γ_c is an angle that defines the direction of the relative velocity vector, and $\hat{\mathbf{v}}_c^w$ is a unit vector in the direction of the wheel velocity with respect to the rail at the contact point, defined as

$$\hat{\mathbf{v}}_c^w = v_c^w\mathbf{t}^w + v_l^w\mathbf{t}_l^w \Big/ \sqrt{\left(v_c^w\right)^2 + \left(v_l^w\right)^2} = \left(\sin\gamma_c\right)\mathbf{t}^w + \left(\cos\gamma_c\right)\mathbf{t}_l^w \tag{30}$$

The angle γ_c is used to define the L/V ratio developed in this study. Recall that $\boldsymbol{\gamma}^w = \overline{\boldsymbol{\gamma}}^w - \mathbf{t}^{w^T}\overline{\boldsymbol{\gamma}}^w\mathbf{t}^w = \mathbf{P}_p^w\overline{\boldsymbol{\gamma}}^w$, which shows that $\boldsymbol{\gamma}^w$ is a vector perpendicular to the climb direction. The friction-force equation $\mathbf{F}_f^w = -F\hat{\mathbf{v}}_c^w = -\mu N\hat{\mathbf{v}}_c^w$ is general and is applicable to both scenarios of wheel climb and sliding-down since it is in a direction opposite to the relative velocity between the wheel and rail. This direction of the relative velocity is defined by the unit vector $\hat{\mathbf{v}}_c^w$.

9. SPATIAL L/V RATIO

It was previously shown that $m^w\ddot{\mathbf{R}}^w = \mathbf{F}_r^w$, where $\mathbf{F}_r^w = \mathbf{P}^w\mathbf{F}^w + m^w\mathbf{P}_p^w\overline{\boldsymbol{\gamma}}^w$ and $\mathbf{P}^w = \mathbf{t}^w \otimes \mathbf{t}^w$. Following the definitions used in developing Nadal's ratio and the definition of the unit vector $\mathbf{b}^r = \mathbf{t}^r \times \mathbf{n}^r$, the lateral force L and the vertical force V can be written as

$$\left.\begin{aligned} L &= \mathbf{n}^{r^T}\left(\mathbf{F}_r^w - \mathbf{F}_f^w\right) = \mathbf{n}^{r^T}\left(\mathbf{F}_r^w - \mu N\hat{\mathbf{v}}_c^w\right) \\ V &= \mathbf{b}^{r^T}\left(\mathbf{F}_r^w - \mathbf{F}_f^w\right) = \mathbf{b}^{r^T}\left(\mathbf{F}_r^w - \mu N\hat{\mathbf{v}}_c^w\right) \end{aligned}\right\} \tag{31}$$

The resultant of the reaction force normal to the contact surface can be written as

$$\begin{aligned} N &= -\mathbf{n}^{w^T}\mathbf{F}_r^w = \mathbf{n}^{w^T}\left(\mathbf{A}^w\begin{bmatrix}F_l & L & -V\end{bmatrix}^T + \mu N\hat{\mathbf{v}}_c^w\right) \\ &= \overline{\mathbf{n}}^{w^T}\begin{bmatrix}F_l & L & -V\end{bmatrix}^T = -L\sin\alpha + V\cos\alpha \end{aligned} \tag{31}$$

In the limiting case used in deriving Nadal's limit, which ignores the effect of $\overline{\boldsymbol{\gamma}}^w$,

$$\begin{aligned} \mathbf{t}^{w^T}\ddot{\mathbf{R}}^w = 0 &= \mathbf{t}^{w^T}\mathbf{F}_r^w = \mathbf{t}^{w^T}\left(\mathbf{A}^w\begin{bmatrix}F_l & L & -V\end{bmatrix}^T + \mu N\hat{\mathbf{v}}_c^w\right) \\ &= \overline{\mathbf{t}}^{w^T}\begin{bmatrix}F_l & L & -V\end{bmatrix}^T + \mu N\sin\gamma_c = -L\cos\alpha - V\cos\alpha + \mu N\sin\gamma_c \end{aligned} \tag{32}$$

The preceding two equations show that

$$\frac{L}{V} = \frac{\sin\alpha - \mu\cos\alpha\sin\gamma_c}{\cos\alpha + \mu\sin\alpha\sin\gamma_c} = \frac{\tan\alpha - \mu\sin\gamma_c}{1 + \mu\tan\alpha\sin\gamma_c} \tag{33}$$

This ratio is derived using the track bank angle that defines the track super-elevation and accounts for the forward motion, angle of attack, and direction of the friction force. This equation is also consistent with the result obtained in [6] using a quasi-static engineering approach. It is obtained in this section as a special case of the three-dimensional dynamic formulation developed in this investigation.

As an example, a flange height of 1.5 in (0.0381 m) is considered. Even if a wheel climb is completed in 2 s, $v_c^w = 0.019$ m/s, which is a low velocity. In case of a vehicle forward velocity

$v_l^w = 20$ m/s (72 km/h), one has $\tan\gamma_c = v_c^w / v_l^w = 8.5\times10^{-4}$. In this case, $\tan\gamma_c \approx \gamma_c = 8.5\times10^{-4}$, and for a flange angle of $72°$, one has $L/V = 3.077$. Increasing the flange angle increases the L/V ratio. For example, for a flange angle $75°$, $L/V = 3.73$; and for a flange angle $77°$, $L/V = 4.33$, demonstrating sensitivity of the L/V limit to changes in the flange angle and validity of concerns regarding its use as the basis for developing derailment criteria, particularly in cases of altered wheel geometry due to wear.

The formulation of the spatial L/V ratio presented in this section allows for investigating the effect of the assumption $\mathbf{t}^{w^T}\ddot{\mathbf{R}}^w = 0$. The vector $\ddot{\mathbf{R}}^w$ can be determined using different climb profiles defined by the function $s^w = s^w(t)$. The solution of the *inverse problem* defines $\ddot{\mathbf{R}}^w$, which depends on both the centrifugal and Coriolis acceleration terms that are dependent on the curve geometry and forward velocity $\dot{s}^r$. Furthermore, because in general $\ddot{\mathbf{R}}^w = -\ddot{s}^w\mathbf{t}^w + \overline{\boldsymbol{\gamma}}^w$ and $\mathbf{t}^{w^T}\ddot{\mathbf{R}}^w = -\ddot{s}^w + \mathbf{t}^{w^T}\overline{\boldsymbol{\gamma}}^w$, the condition that $\mathbf{t}^{w^T}\ddot{\mathbf{R}}^w = 0$ does not imply always that $\ddot{s}^w$ is zero as in the planar analysis. One can show that in the spatial analysis, $\mathbf{t}^{w^T}\ddot{\mathbf{R}}^w = 0$ leads to $\ddot{s}^w = \mathbf{t}^{w^T}\overline{\boldsymbol{\gamma}}^w = (\dot{\psi})^2\,\mathbf{t}^{w^T}\left[\mathbf{A}_{sd}^w\overline{\mathbf{u}}_c^w - \mathbf{R}^r\right]$. Because $\mathbf{t}^{w^T}\mathbf{R}^r = R^r\cos\alpha$ in the case of small track super-elevation angle ϕ^r, this condition can be written as

$$\ddot{s}^w = \mathbf{t}^{w^T}\overline{\boldsymbol{\gamma}}^w = (\dot{\psi})^2\left[\mathbf{t}^{w^T}\mathbf{A}_{sd}^w\overline{\mathbf{u}}_c^w - R^r\cos\alpha\right] \tag{34}$$

This condition states that, when $\ddot{\mathbf{R}}^w = \mathbf{0}$, the climb acceleration $\ddot{s}^w$ is equal to the component of the centrifugal acceleration along the wheel flange. The fact that this condition can be rarely satisfied during the wheel climb raises concerns with regard to using the L/V ratio in accident investigations. If, on the other hand, $\ddot{s}^w = 0$, one has $\ddot{\mathbf{R}}^w = \overline{\boldsymbol{\gamma}}^w = (\dot{\psi})^2\left[\mathbf{A}_{sd}^w\overline{\mathbf{u}}_c^w - \mathbf{R}^r\right] - 2\dot{s}^w\dot{\psi}\mathbf{A}_{\psi}^w\overline{\mathbf{t}}^w$

, and this term can be included in the longitudinal, lateral, and vertical force to define the L/V ratio. Nonetheless, the condition $\ddot{s}^w = 0$ cannot be ensured during the wheel climb.

10. SUMMARY

While wheel climb has been a source of many railroad accidents, simple analysis based on quasi-static planar analysis is often used to provide explanation for the climb phenomenon [17, 18]. In particular, Nadal's L/V limit has been used for developing several railroad derailment criteria often used in accident investigations and in developing operation and safety guidelines. This is despite the fact that such a limit is based on quasi-static planar analysis. A new spatial dynamic formulation of the L/V ratio is developed in this study using the basic assumptions adopted in developing Nadal's limit. The three-dimensional analysis, which leads to minor modification of Nadal's L/V limit, demonstrates the limitations of the planar analysis. The spatial L/V ratio, derived using *non-generalized coordinates*, is independent of the bank angle that defines the track super-elevation, accounts for curving behavior, track super-elevation, and centrifugal and Coriolis inertia forces. The spatial analysis presented in this study demonstrates the dependence of the lateral and vertical forces on the quadratic-velocity inertia forces and that the wheel absolute acceleration is not in general zero when the climb acceleration is zero as in the planar analysis. It is shown that the L/V limit can approach high values if the direction of the friction force is properly accounted for, highlighting the need for accurate measurement of the wheel/rail relative velocity and its direction for proper interpretation and use of the L/V limit. The single-degree-of-freedom model defined in this study based on spatial formulation can be used to define an *inverse problem* for the study of different climb patterns. Furthermore, such a model can be used for developing real-time PTC onboard-computer algorithms that utilize online measurements to

define, from the outset, a wheel-climb pattern. Using measured accelerations, the PTC algorithms can compute in real-time the climb acceleration, velocity, and displacement; which when properly used with control actions, can contribute to avoiding wheel-climb derailments during curving.

REFERENCES

1. Wang, W., and Li, G.X., 2010, "Development of Simulation of a High Speed Vehicle for a derailment Mechanism", *IMechE Journal of Rail and Rapid Transit*, Vol. 224, pp. 103 – 113.
2. Zeng, J., and Wu, P., 2008, "Study on the Wheel/Rail Interaction and Derailment Safety", *Wear*, Vol. 265, pp. 1452 – 1456.
3. Shabana, A.A., 2012, "Nadal's Formula and High Speed Rail Derailments", *ASME Journal of Computational and Nonlinear Dynamics*, Vol.7, pp. 41003-1 – 41003-8.
4. Blader, F.B., 1990, "A Review of Literature and Methodologies in the Study of derailment Caused by Excessive Forces at the Wheel/Rail Interface", AAR Report R-717, Association of American Railroads, Washington, D.C.
5. Elkins, J., and Wu, H., 2000, "New Criteria for Flange Climb Derailment", IEEE/ASME Joint Rail Conference, Newark, New Jersey, April 4-6, 2000.
6. Marquis, B., and Grief, R., 2011, "Application of Nadal Limit in the Prediction of Wheel Climb Derailment", Proceedings of the ASME/ASCE/IEEE 2011 Joint Rail Conference, Pueblo, Colorado, Paper # JRC2011-56064, March 16-18, 2011.
7. Shust, W.C., Elkins, J.A., Kalay, J.A., and El-Sibaie, M., 1997, "Wheel Climb Derailment Tests Using AAR's Track Loading Vehicle", Association of American Railroads Report R-910.
8. Wu, H., and Elkins, J., 1999, "Investigation of Wheel Flange Climb Derailment Criteria" Association of American Railroads Report R-931.
9. Wilson, N., Shu, X., and Kramp, K., 2004, "Effect of Independently Rolling Wheels on Flange Climb Derailment", Proceedings of the ASME International Mechanical Engineering Congress.

10. Weinstock, H., 1984, “Wheel Climb Derailment Criteria for Evaluation of Rail Vehicle Safety”, Proceedings of the ASME Winter Annual Meeting, 84-WA/RT-1, New Orleans, LA.
11. Matsudaria, T., 1963, “Dynamics of high Speed Rolling Stock”, Japanese National Railways RTRI Quarterly Reports, Special issue.
12. Koci, H.H., and Swenson, C.A., 1978, “Locomotive Wheel Loading – A System Approach”, General Motors Electromotive Division, LaGrange, IL.
13. Nadal, M.J., 1908, Locomotives á Vapeur, Collection Encyclopédie Scientifique, Bibliotéque de Mécanique Appliquée et Génie, Vol. 186, Paris.
14. Shabana, A.A., and Sany, J.R., 2001, “An Augmented Formulation for Mechanical Systems with Non-Generalized Coordinates: Application to Rigid Body Contact problems”, *Nonlinear Dynamics*, Vol. 24, No. 2, 2001, pp. 183-204.
15. Shabana, A.A., 2021, *Mathematical Foundation of Railroad Vehicle Systems: Geometry and Mechanics*, John Wiley & Sons, Chichester, UK.
16. Shabana, A.A., Zaazaa, K.E., and Sugiyama, H., 2008, *Railroad Vehicle Dynamics: A Computational Approach*, CRC/Taylor & Francis.
17. O’Shea, J.J., Shabana, A.A., “Analytical and Numerical Investigation of Wheel Climb at Large Angle of Attack”, *Nonlinear Dynamics*, Vol. 83, 2016, pp. 555 - 577.
18. O’Shea, J.J., Shabana, A.A., “Further Investigation of Wheel Climb Initiation: Three-Point Contact”, *IMechE Journal of Multibody Dynamics*, Vol. 231, 2017, pp. 121 – 132, DOI: 10.1177/1464419316654402.

List of Figures

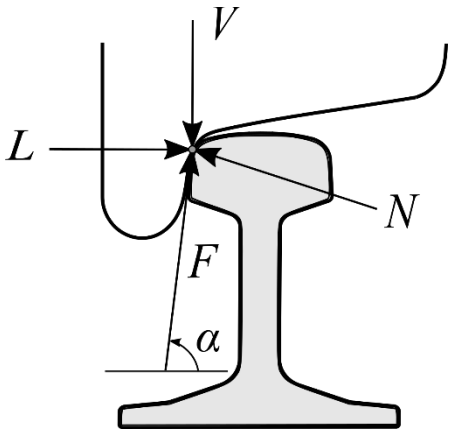

Figure 1 Nadal's force balance [15]